The 1908 Tunguska explosion: atmospheric disruption of a stony asteroid

Christopher F. Chyba[*†], Paul J. Thomas[‡] & Kevin J. Zahnle[*]

* Space Science Division, MS 245-3, NASA Ames Research Center, Moffett Field, California 94035, USA
‡ Department of Physics and Astronomy, University of Wisconsin, Eau Claire, Wisconsin 54702, USA

The explosion over Tunguska, Central Siberia, in 1908 released 10 to 20 megatons (high explosive equivalent) of energy at an altitude of about 10 km. This event represents a typical fate for stony asteroids tens of metres in radius entering the Earth's atmosphere at common hypersonic velocities. Comets and carbonaceous asteroids of the appropriate energy disrupt too high, whereas typical iron objects reach and crater the terrestrial surface.

THE explosion[1-5] on 30 June 1908 over Tunguska has inspired many exotic explanations. Antimatter[6], a small black hole[7] and, inevitably, an exploding flying saucer[2], have all been proposed as means of liberating tens of megatons of energy in the atmosphere without cratering the Earth's surface. Quantitative explanations in terms of a less exotic object have often suggested that it must have been extremely underdense (with an effective density $\rho_m \approx 10^{-3}$–10^{-2} g cm^{-3}) to have exploded before reaching the ground[8-12]. Contrary to that claim, we show that the Tunguska explosion is a typical fate for stony asteroids with radii ~ 30 m entering the Earth's atmosphere at common hypersonic velocities. Short-period and long-period comets with appropriate energies explode far too high in the atmosphere to account for the observations, whereas iron objects (with rare exceptions) explode too low, or not at all. Our model is also consistent with the fate of the Revelstoke object, observed[13] to have catastrophically exploded in the atmosphere with an energy of tens of kilotons[4]. These results affect assessments of the hazard posed by impacts of small comets and asteroids.

Characteristics of the Tunguska event

The Tunguska event has been variously estimated as liberating between 4×10^{23} (ref. 14) and 4×10^{25} erg, (ref. 12) or 10–10^3 megatons (Mton). The best energy estimates are based on air and seismic wave records, compared with nuclear airbursts of comparable yield. Hunt et al.[14] thereby find an explosive energy of 10 ± 5 Mton; a more recent analysis by Ben-Menahem[15] finds 12.5 ± 2.5 Mton. Similar estimates derive from observed forest destruction, scaled from the uprooting of trees in nuclear weapons tests[14,16].

Seismic waves were excited by a vertical point impulse of 7×10^{18} dyn s (ref. 15). The impulse has been interpreted[12] as the initial vertical momentum of the impactor, which implies a bolide kinetic energy of $\sim 4 \times 10^{25}$ erg. This interpretation is problematic, as the impulse striking the ground is largely from the blast wave generated by the explosion, and not due to the detached ballistic shock from the decelerated impactor[15]. Turco et al.[12] distinguish between the Tunguska terminal explosion and energy released by ablation and deceleration during atmospheric entry, with the explosion representing just the last 1% of the bolide's energy. This requires the bolide to be extremely underdense ($\rho_m < 0.01$ g cm^{-3}) by the time it enters the upper atmosphere.

A reported[17] iridium spike coincident with Tunguska in Antarctic ice corresponds to an impactor with energy $\geqslant 10^{25}$ erg. New analyses on Antarctic samples, however, have found no detectable iridium imprint above background due to cosmic dust, contradicting the earlier result[18]. No evidence for pre-

dicted[12] elevated nitrate production has been found in a greenland ice core[19].

Contrary to interpretations of the Tunguska object as a friable, underdense comet, Sekanina[20] favours a bolide with a very high strength, arguing that the object would explode instantly on disruption. Levin and Bronshten[21] reach similar conclusions, by analogy with typical terminal-flare meteors. Shoemaker[4] asserts that Tunguska-like explosions should be a common fate of small bolides entering the terrestrial atmosphere, provided only that they are less strong than iron objects.

The terminal explosion over Tunguska is typically estimated to have occurred at roughly an atmospheric scale height $H \approx 8.4$ km. Ben-Menahem[15] has compared differing arrival times for Rayleigh and SH body waves recorded at Irkutsk; he finds an explosion height of 8.5 km. This agrees with simulations[16,22] of the treefall pattern, which suggests explosion altitudes of 5–10 km.

The inclination angle θ (measured from the horizontal) of the Tunguska object's trajectory has been controversial. Attempts[3,20,21] to determine θ from eyewitness reports typically give shallow trajectories, in the range 5–17°. Such low inclinations are inconsistent with attempts to simulate the treefall pattern at the Tunguska site. Zotkin and Tsikulin[23] measured the azimuths of 40,000 felled tree trunks over 2,200 km^2 at the Tunguska site, and reproduced the observed 'butterfly' pattern in the laboratory by superimposing a terminal point charge and an inclined line charge. Their investigations require $10° < \theta < 60°$, with a preferred value of 30°. Korobeinikov et al.[22] simulated the treefall pattern using a numerical shock model, finding that observations can be matched only for $30° < \theta < 45°$, with a preferred value of 40°. They further assert that this value is consistent with eyewitness accounts.

Evidently it is difficult to determine the true inclination of the Tunguska bolide, and eyewitness reports gathered 20 years after the event are particularly suspect. In this investigation, we usually take θ to be the most probable entry angle for an incident object, 45°, but consider a range of other possible values.

Atmospheric entry of the bolide

A cosmic object entering the atmosphere loses its kinetic energy through deceleration and ablation[24-26]. Deceleration can be described by the equation

$$m\frac{dv}{dt} = -\tfrac{1}{2}C_D\rho_a Av^2 + \frac{g}{m}\sin\theta \qquad (1)$$

where r is the bolide's radius, A its cross-sectional area, ρ_a atmospheric density, g gravitational acceleration (a function of height), t time, and C_D drag coefficient. The object's surface is heated by radiation from the atmospheric shock front. This heat is shed efficiently by ablation. The resulting change in mass is

given by

$$Q\frac{dm}{dt} = -\tfrac{1}{2}C_H\rho_a A v^3 \qquad (2)$$

where Q is the heat of ablation and C_H is the heat transfer coefficient. Q is a function of material type and the specific process of ablation. To derive the values of Q used here, we begin with the heat of vaporization appropriate to iron and stony meteorites[24], 8×10^{10} erg g^{-1}. We then use observed ablation coefficients for cometary, carbonaceous and stony meteors to calculate Q for comets and carbonaceous asteroids, following Chyba et al.[27] (see Table 1).

Observation indicates[25] that C_H is effectively constant at $C_H \approx 0.1$ above ~30 km. This altitude range includes most visible meteors. But as a bolide descends to lower altitudes, C_H declines inversely with atmospheric density, so that $\dot{m}$, which had been increasing, becomes effectively constant. This upper limit on $\dot{m}$ occurs because large objects ablate mainly by absorbing thermal radiation emitted by the hot, shocked gases concentrated in front of the impactor. The temperature attained by the shocked gas is strongly regulated by thermal ionization[28,29] to ~25,000–30,000 K, with weak dependence on the velocity, size and composition of the impactor. The maximum ablation rate is therefore $Q\dot{m} \approx A\sigma T^4$. These considerations suggest rewriting equation (2) as[29]

$$Q\frac{dm}{dt} = -A \min\left(\tfrac{1}{2}C_H^0\rho_a v^3,\ \sigma T^4\right) \qquad (3)$$

where $C_H^0 = 0.1$ and $T = 25,000$ K. This parametrization roughly reproduces the results of ref. 30.

The bolide's trajectory angle θ varies as

$$\frac{d\theta}{dt} = \frac{g\cos\theta}{v} - \frac{C_L\rho_a A v}{2m} - \frac{v\cos\theta}{R_\oplus + h} \qquad (4)$$

Here $R_\oplus$ is the Earth's radius, h the bolide's height above the terrestrial surface, and C_L the lift coefficient. Passey and Melosh[31] suggest taking $C_L \lesssim 10^{-3}$, on the basis of their investigations of crater fields. We set $C_L = 10^{-3}$. Even for trajectories as low as $\theta = 15°$, varying C_L over the range 10^{-3}–1 changes the altitude at which a Tunguska-sized stony asteroid airbursts by only ~1%.

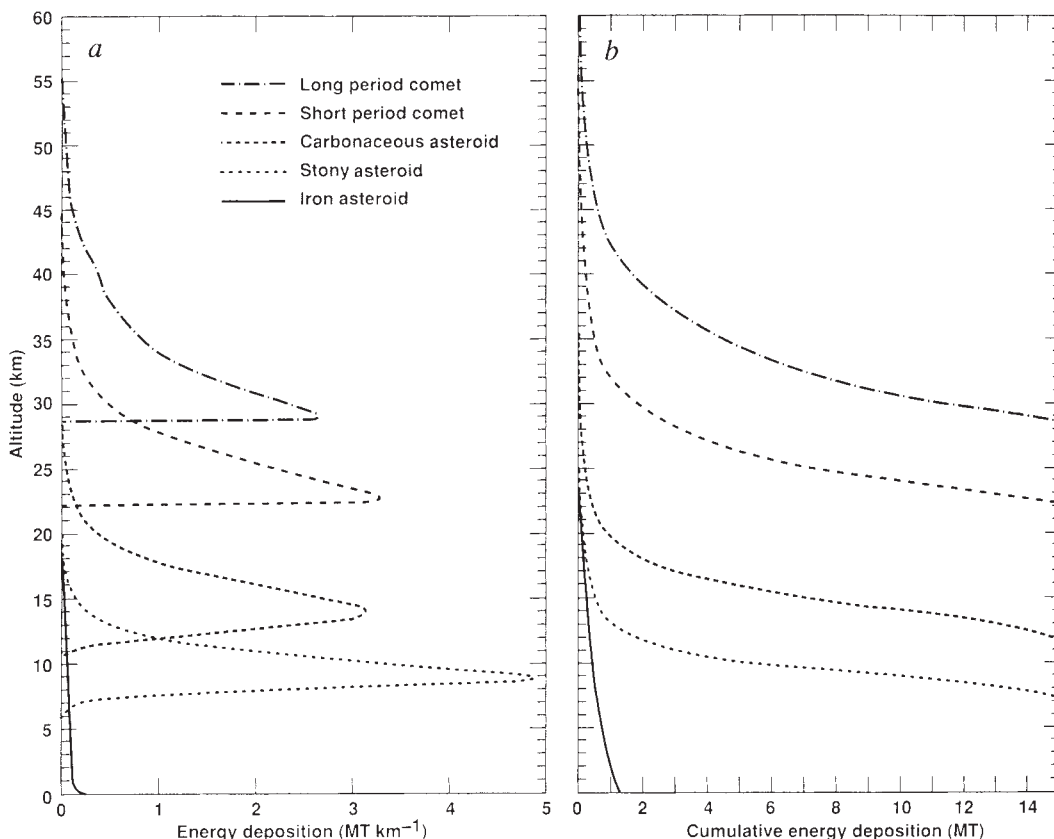Equations (1) and (2) can be solved analytically for spherical impactors in an isothermal atmosphere if θ and C_H are held constant[25]. The analytical solution does not, however, allow for objects breaking up in response to aerodynamic forces. We therefore apply a finite-difference approach to solving the required equations.

Catastrophic fragmentation

Catastrophic fragmentation is a likely means of producing an atmospheric explosion of a bolide. By spreading the impactor's mass over a wide area, fragmentation increases the amount of atmosphere intercepted and so enhances ablation and aerobraking; hence a fragmenting object stops more abruptly, surrendering its kinetic energy more explosively, than does a non-fragmenting object[21,31,32].

Objects much greater than ~1 km in diameter do not fragment while traversing the Earth's atmosphere, as an atmospherically induced pressure wave has insufficient time to cross the object before impact. In effect, large objects moving at hypersonic velocities do not have time to 'see' the atmosphere before cratering the surface[27]. (This is consistent with the existence of the 14-km-wide Lappajärvi crater in Finland, apparently the result of an impactor of carbonaceous chondritic composition[33]; this crater would have been excavated by a carbonaceous asteroid ~1 km in diameter.) Sufficiently small objects will either be entirely ablated, or be aerobraked to free-fall speeds. Atmospheric entry of objects in the size range ~10–100 m, however, is dominated by fragmentation, although the precise size range depends strongly on object type and velocity.

FIG. 1 Airburst altitudes for five 15-Mton candidate Tunguska bolides incident at 45°. Comets and carbonaceous asteroids deposit their energy too high in the atmosphere to account for the Tunguska explosion, whereas iron objects reach and crater the surface. Typical stony asteroids, however, deliver the bulk of their energy near an altitude of 9 km, and this is consistent with observations.

Deformation and fragmentation occur because of differential atmospheric pressure across the object. The leading face of the impactor is subjected to an average pressure $p_s \approx C_D \rho_a v^2 / 2$, whereas the pressure on the trailing face is much smaller. Integrated over the surface of the impactor, this difference produces the drag force of equation (1). Pressures on the side of the objects are also much smaller[34] than p_s, so that the object is essentially not laterally confined. Impactors fragment as the result of this aerodynamic stress[24,25,31,35,36]. Fragmentation occurs when p_s exceeds a characteristic strength of the material. Because the details of bolide failure are poorly understood[24], we select characteristic strengths for various bolides using the following considerations.

Fragmentation of 'Sun-grazing' and 'Jupiter-grazing' comets, presumably due to tidal stresses, suggests[37] that at least some comets may have extremely low tensile strengths of 10^3–10^5 dyn cm^{-2}. Objects have fragmented in the terrestrial atmosphere with strengths[25] as low as 6×10^5 dyn cm^{-2}. A typical strength of a chondritic impactor is 1×10^7 to 5×10^7 dyn cm^{-2}, although stronger stony objects can have strengths[25] as high as 2×10^7–5×10^8 dyn cm^{-2}. By contrast iron bodies are strong and usually do not fragment until they penetrate to $\lesssim 10$ km of the ground. The effective strength for an iron impactor[25] is 4×10^8–2×10^9 dyn cm^{-2}. For an object entering the atmosphere at 20 km s^{-1}, aerodynamic stresses reach $\sim 6 \times 10^8$ dyn cm^{-2} two scale heights up, exceeding most of the strengths cited above.

A model for bolide deformation

A right circular cylinder moving along its axis of symmetry makes a highly idealized but straightforward model of a deforming impactor. To represent a roughly equidimensional bolide, we choose a 'cubical' cylinder, taking its height h and diameter $2r$ to be initially equal. We now consider the forces on the cylinder as it passes through the atmosphere. The front face sees a pressure $p_s = C_D \rho_a v^2 / 2$. For a cylinder[38], $C_D \approx 1.7$. Provided that the sound travel time h/c (c is the sound speed in the object) is short compared with the time $H \csc \theta / v$ for the impactor to fall through a scale height, stresses parallel to the axis should roughly be in hydrostatic equilibrium, with the axial stress at any point within the object being that required to decelerate the trailing mass. Thus the axial stress decreases linearly from its peak value p_s at the front face to some low value $\ll p_s$ at the rear face.

The air pressure against the side walls is generally much less[34] than p_s and except near the back of the cylinder is small compared with the axial stress. As the cylinder descends into deeper air, axial stress increases until elastic failure occurs. The cylinder flows outward, transversely to the direction of motion. Because the driving pressure p_s rises exponentially as the bolide descends through the atmosphere, its effective cross-section increases exponentially with time. A real disrupting cylinder would fail first at its leading edge, where pressures are highest. The locus of failure thereafter moves backwards into the cylinder. Because the pressures are always highest at the front the expansion is

always fastest there, although the most rapidly expanding elements may be swept away by the flow.

As a first approximation, we assume that the cylinder deforms globally to become a squatter version of itself. The average interior pressure is $p_s/2$. Neglecting the confining air pressure against the side walls, and assuming that the material strength of the cylinder has been exceeded, a global approximation to the force balance on the side walls is

$$(2\pi rh)(\tfrac{1}{4}C_D \rho_a v^2) \approx m \frac{d^2 r}{d t^2} \qquad (5)$$

where the inertial mass is identified with the mass m of the cylinder. Assuming that the density ρ_m of the disrupted cylinder remains constant, h and m can be eliminated from equation (5), to give

$$r \frac{d^2 r}{d t^2} = \frac{C_D \rho_a v^2}{2 \rho_m} \qquad (6)$$

This equation is functionally identical (differing by only a factor of order unity) to the analogous equation derived by Zahnle[29] using a wholly different argument. Our finite-difference scheme solves equations (1)–(4) numerically, beginning at an altitude of 100 km, and calculating the decrease in altitude dh over a time interval dt according to $dh = -(v \sin \theta) \, dt$. The atmospheric density ρ_a is determined at each timestep by exponential interpolation from standard atmosphere tables[39]. Once the central pressure $C_D \rho_a v^2 / 4$ exceeds the object's strength, equation (6) is used to calculate the changing radius r and effective cross-section $A = \pi r^2$.

Numerical results

Eight 'Tunguska bolides' are listed in Table 1. All cases correspond to an initial kinetic energy at $h = 100$ km of 15 Mton. (Objects lose different fractions of their kinetic energy before catastrophic disruption; for example, the 29-m stony asteroid entering at $45°$ has had its kinetic energy reduced by ablation and deceleration to ~ 10 Mton by the time it reaches 10 km altitude.) We compare five object types (iron, stony and carbonaceous asteroids; and short- and long-period comets), and, for stony asteroids, four incidence angles ($15°$, $30°$, $45°$ and $90°$). All other objects are incident at $\theta = 45°$. The three asteroids have initial velocities of 15 km s^{-1}, the median impact velocity for Earth-crossing asteroids[40]. Incident comet velocities are 25 km s^{-1} and 50 km s^{-1} for the short-period and long-period cases, respectively; again these are approximate median values[40,41]. Both comets are assumed to have strengths of 10^6 dyn cm^{-2}, one-tenth that of the carbonaecous body.

Figure 1 compares energy release curves for the five kinds of object at $\theta = 45°$. Figure 1a shows the altitude profile of energy release in units of Mton high explosive equivalent per kilometre. The two comets are entirely ablated, whereas the stony objects lose most of their kinetic energy to deceleration, not ablation. Figure 1b shows cumulative energy loss (Mton) along the object's path above the indicated altitude.

TABLE 1   Possibilities considered for the 15-Mton Tunguska object

Object type	Density (g cm^{-3})	Mass (g)	Radius (m)	Velocity (km s^{-1})	Heat of ablation (erg g^{-1})	Yield strength (dyn cm^{-2})	θ	Airburst height (km)
Iron	7.9	5.6×10^{11}	22	15	8×10^{10}	1×10^9	$45°$	0
Stone	3.5	5.6×10^{11}	29	15	8×10^{10}	1×10^8	$45°$	9
Carbonaceous	2.2	5.6×10^{11}	34	15	5×10^{10}	1×10^7	$45°$	14
SP comet	1.0	2.0×10^{11}	32	25	2.5×10^{10}	1×10^6	$45°$	23
LP comet	1.0	5.0×10^{10}	20	50	2.5×10^{10}	1×10^6	$45°$	29
Stone	3.5	5.6×10^{11}	29	15	8×10^{10}	1×10^8	$15°$	15
Stone	3.5	5.6×10^{11}	29	15	8×10^{10}	1×10^8	$30°$	11
Stone	3.5	5.6×10^{11}	29	15	8×10^{10}	1×10^8	$90°$	6

SP, short-period; LP, long-period.

Where the curves in Fig. 1a peak, objects have typically spread to ~5–10 times their initial linear dimensions. This greatly enhances both ablation and deceleration, but it is misleading, because equation (2) ceases to be valid before an object has spread to this extent. Equation (2) assumes that the fragments of the disrupted object may continue to be treated with a single, collective bow shock. At some point the object spreads sufficiently for this approximation to break down, and the collective bow shock dissolves into separate bow shocks as the fragments accelerate away from one another[31]. This effect is presumably what produces crater-strewn fields[31]. It is not clear at what (spreading) radius greater than a bolide's initial radius the collective bow-shock approximation breaks down. This ambiguity does not greatly alter our conclusions regarding airburst altitude: once an object has spread to, say, twice its initial radius, its further spreading happens so quickly that an 'explosion altitude' is defined to within a few kilometres, regardless of whether the explosion is taken to occur then or when the object has spread to 5–10 times its initial radius.

The weak, fast-moving, easily ablated comets do not penetrate the atmosphere very deeply. Neither approaches the altitude of the Tunguska explosion. Even if the comets had strengths comparable to that of stony asteroids, they still could not fit the Tunguska observations. For example, giving the short-period comet a strength of 1×10^8 dyn cm^{-2} leads to complete ablation by an altitude of 16 km. Nor does assigning a 15-Mton incident comet an anomalously low asteroid-like velocity of 15 km s^{-1} allow it to penetrate below ~16 km before it is completely ablated. Moreover, comets may be less dense than the 1 g cm^{-3} value chosen here; values as low as $\rho_m \approx 0.3$ g cm^{-3} may be possible[42]. Such lower-density objects would airburst even higher.

The carbonaceous object, stronger and slower than the comets, penetrates more deeply, but also explodes at too high an altitude. If this carbonaceous bolide were to enter the atmosphere at $\theta = 60°$, however, it would airburst at an altitude of 11–12 km.

These parameters are at the limits of those allowed by treefall simulations[16,22]. Similarly, granting a carbonaceous object the strength of a stony asteroid would allow it to penetrate to comparable altitudes. Therefore a carbonaceous asteroid, although unlikely, cannot be ruled out as an explanation of the Tunguska event.

The stronger, denser, stony object in Table 1 penetrates to ~9 km above the ground, consistent with the Tunguska airburst altitude. Figure 2 shows the effect of impact angle on the explosion of stony asteroids. Results for four initial values of θ, 15°, 30°, 45° and 90° are given. The more nearly vertical an object's trajectory, the deeper it penetrates into the atmosphere before catastrophic disruption. Values of θ much less than 30° seem to be inconsistent with an explanation of the Tunguska object as a stony asteroid.

The most probable fate for a 15-Mton iron object is impact with the ground. Its high density (small cross-section) and high strength favour its survival. However, 15-Mton iron objects with speeds much in excess of the median value of 15 km s^{-1} will airburst before impact. Our simulations indicate that, although it is possible for such an iron object to reproduce the Tunguska event, an encounter speed in the range ~30–40 km s^{-1} is required. This excludes ~90% of known Earth-crossing asteroid orbits[40]. These results are only weakly dependent on θ.

In summary, Tunguska was probably a fairly strong, dense, asteroid-like object, but probably not as strong or dense as iron. Carbonaceous asteroids and especially comets are unlikely candidates for the Tunguska object.

'Light nights' over Eurasia

Widespread 'light nights' were observed[3] over Eurasia for the first few nights after the Tunguska event. Turco et al.[12] suggest three possible explanations: nightglow from NO_x-O_x reactions; dust; and noctilucent water clouds. The latter require injection or deposition at altitudes >50 km to take advantage of the strong easterly winds needed to account for the observed geographical
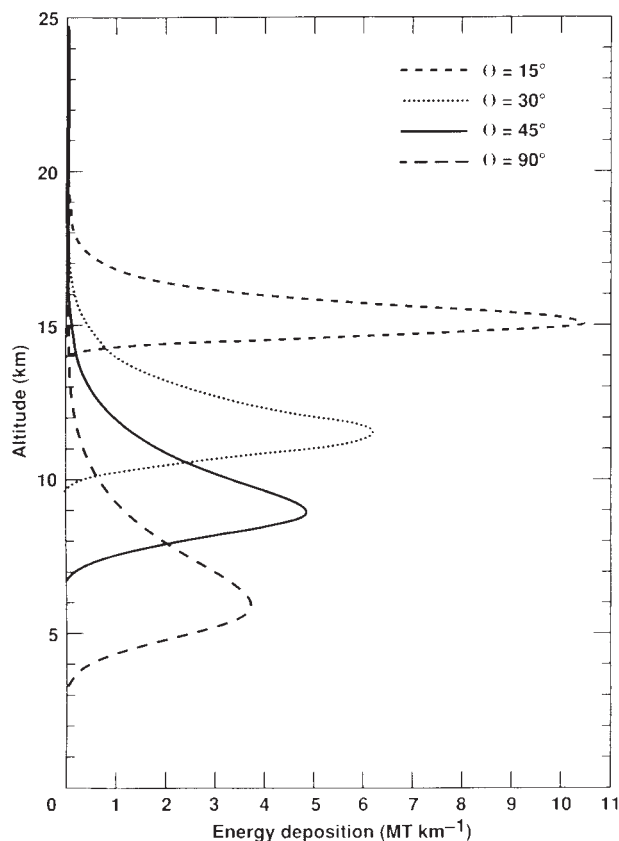

FIG. 2 Airburst altitudes for four 15-Mton stony asteroids with different incidence angles. The more nearly vertical an object's trajectory, the deeper it penetrates into the atmosphere before catastrophic disruption.

range of the phenomenon[12]. The effect has also been attributed[8] to the putative comet's tail, a less plausible explanation[12].

Tunguska was a ~15-Mton airburst at an altitude of roughly a scale height. The effects of explosion blast waves scale as the ratio of blast energy to atmospheric density[43]. We therefore expect the Tunguska fireball to have reached a height above its airburst altitude appropriate to a ~$15e \approx 40$ Mton nuclear surface burst. The fireball for a 40-Mton surface burst rises to an altitude[43] of ~40 km. A rough estimate of the amount of water that could have been entrained by this fireball is $\pi R^2 H \rho_{H_2O}$, where R is the radius of the fireball when its pressure has dropped to the ambient value (several kilometres for a 10-Mton nuclear blast[44]), and ρ_{H_2O} the density of atmospheric water vapour (several times $10^{-3} \rho_a$). The result, ~10^{35} molecules H_2O injected to ~50 km altitude, seems sufficient for noctilucent clouds to be produced[12]. The Tunguska explosion may have lofted enough material high enough to account for the European 'light nights'.

Other impacts and recent airbursts

The model developed here for the Tunguska explosion may be tested for consistency with Meteor Crater in Arizona, and with the Tunguska-like explosions of the Revelstoke, Kincardine and other bolides. We consider these in turn.

Meteor Crater. Meteor Crater in Arizona was excavated ~10^4 yr ago by an iron object with a kinetic energy[4] of ~15 Mton. Our model predicts that such an object disrupts so close to the surface that its fragments crater the surface as if from a coherent object, consistent with the appearance of Meteor Crater.

Revelstoke. In March 1965 a small bolide travelling at $\theta \approx 15°$ exploded 30 km above Revelstoke, Canada[13], with an energy in the tens of kiloton range[4]. Examination of recovered material shows it to have been a type I carbonaceous chondrite[13]. (Largely unprocessed ~1 mm sized fragments were recovered from the Revelstoke site[13]; only spherules of vaporized and recondensed material were recovered in the case of Tunguska[3]. Siderophile abundances in these spherules are consistent with extraterrestrial origin from a single object[17], but are insufficient to determine the type of the Tunguska object. No scientific expeditions

reached the Tunguska site until almost 20 years after the event; it is not surprising that no other remnants of the object were found.) Microbarograph estimates of the explosive energy of the Revelstoke object range from 20 kton (ref. 4) to 70 kton (ref. 45).

We model Revelstoke as a carbonaceous chondrite (as in Table 1), moving at 15 km s^{-1} with an initial kinetic energy of 20 kton (corresponding to a cylinder of initial radius $r = 3.8$ m) and $\theta = 15°$. Our simulation shows that such an object's strength is exceeded at an altitude of ~33 km, giving maximum kinetic energy deposition to the atmosphere at ~32 km.

Kincardine and other bolides. The Kincardine and College objects exploded over Ontario in 1966 and Alaska in 1969, respectively, each at altitudes just over 60 km. Explosive energies in the kiloton to megaton range are possible[45]. These objects therefore provide only weak constraints on our model. Our model does predict that long-period comets with kinetic energies in the tens of kiloton range should catastrophically disrupt and deposit the bulk of their energy just above 60 km altitude, so the fates of these objects are consistent with cometary airbursts.

The fates of bolides

The simple model for bolide deformation and catastrophic disruption presented here is consistent with the fates and explosive energies of the Meteor Crater, Tunguska and Revelstoke objects, provided that these objects were iron, stony and carbonaceous asteroids, respectively. The Meteor Crater and Revelstoke bolides are in fact known from recovered material to have had these identities. Within broad uncertainties, the explosions of the Kincardine and College objects are consistent with the fates of long-period comets with kinetic energies of tens of kilotons.

The fate of bolides in the Tunguska size range is strongly dependent on the nature of the object. Had the Tunguska object been a 15-Mton comet, far less surface destruction would have resulted, because of the much higher altitude of the airburst. Comets incident with tens of kilotons of energy explode so high in the atmosphere that they are scarcely noticed at the surface. Denser objects with higher material strengths are therefore necessarily more dangerous to surface life. □

Received 22 September; accepted 9 December 1992.

1. Kulik, L. A. *Dokl. Acad. Nauk SSSR* **23**, 399–402 (1927).
2. Baxter, J. & Atkins, T. *The Fire Came By* (Doubleday, Garden City NY, 1976).
3. Whipple, F. J. W. *Q.Jl R. met. Soc.* **56**, 287–304 (1930).
4. Krinov, E. L. *Giant Meteorites* (Pergamon, Oxford, 1966).
5. Shoemaker, E. M. *A. Rev. Earth planet. Sci.* **11**, 461–494 (1983).
6. Cowan, C., Atluri, C. R. & Libby, W. F. *Nature* **206**, 861–865.
7. Jackson, A. A. & Ryan, M. P. *Nature* **245**, 88–89 (1973).
8. Fesenkov, V. G. *Sov. Astr.* **5**, 441–451 (1962).
9. Petrov, G. I. & Stulov, V. P. *Cosmic Res.* **13**, 525–531 (1975).
10. Liu, V. C. *Geophys. Res. Lett.* **5**, 309–312 (1978).
11. Park, C. *Acta astronaut.* **5**, 523–542 (1978).
12. Turco, R. P. *et al. Icarus* **50**, 1–52 (1982).
13. Folinsbee, R. E., Douglas, J. A. V. & Maxwell, J. A. *Geochim. cosmochim. Acta* **31**, 1625–1635 (1967).
14. Hunt, J. N., Palmer, R. & Penney, W. *Phil. Trans. R. Soc. Lond.* **252**, 275–315 (1960).
15. Ben-Menahem, A. *Phys. Earth planet. Int.* **11**, 1–35 (1975).
16. Zolotov, A. V. *Sov. Phys. Dokl.* **12**, 101–104 (1967).
17. Ganapathy, R. *Science* **220**, 1158–1161 (1983).
18. Rocchia, R. *et al.* in *Global Catastrophes in Earth History* (eds Sharpton, V. L. & Ward, P. D.), 189–193 (Geol. Soc. Am. SP-247, Boulder CO, 1990).
19. Neftel, A., Beer, J., Oeschger, H., Zücher, F. & Finkel, R. C. *Nature* **314**, 611–613 (1985).
20. Sekanina, Z. *Astr. J.* **88**, 1382–1414 (1983).
21. Levin, B. Yu. & Bronshten, V. A. *Meteoritics* **21**, 199–215 (1986).
22. Korobeinikov, V. P., Chushkin, P. I. & Shurshalov, L. V. *Acta astronaut.* **3**, 615–622 (1976).
23. Zotkin, I. T. & Tsikulin, M. A. *Sov. Phys. Dokl.* **11**, 183–186 (1966).
24. Baldwin, B. & Sheaffer, Y. *J. geophys. Res.* **76**, 4653–4668 (1971).
25. Bronshten, V. A. *Physics of Meteoric Phenomena* (Reidel, Dordrecht, 1983).
26. Melosh, H. J. *Impact Cratering* (Oxford Univ. Press, New York, 1989).

27. Chyba, C. F., Thomas, P. J., Brookshaw, L. & Sagan, C. *Science* **249**, 366–373 (1990).
28. Walker, J. C. G. *Icarus* **68**, 87–98 (1986).
29. Zahnle, K. J. *J. geophys. Res.* **97**, 10,243–10,255 (1992).
30. Biberman, L. M., Bronin, S. Ya. & Brykin, M. V. *Acta astronaut.* **7**, 53–65 (1980).
31. Passey, Q. R. & Melosh, H. J. *Icarus* **42**, 211–233 (1980).
32. Grigoryan, S. S. *Cosmic Res.* **17**, 724–740 (1979).
33. Grieve, R. A. F. in *Geological Implications of Impacts of Large Asteroids and Comets on the Earth* (eds Silver, L. T. & Schultz, P. H.) 25–37 (Geol. Soc. Am. SP-190, Boulder CO, 1982).
34. Seiff, A. in *Gas Dynamics in Space Exploration*, 19–32 (NASA SP-24, 1962).
35. Öpik, E. J. *Physics of Meteor Flight in the Atmosphere* (Interscience, New York, 1958).
36. Ivanov, B. A., Basilevsky, A. T., Kryuchkov, V. P. & Chernaya, I. M. *J. geophys. Res.* **91**, D413–D430 (1986).
37. Sekanina, Z. in *Comets* (ed. Wilkening, L. L.), 251–287 (Univ. of Arizona, 1982).
38. Hoerner, S. F. *Fluid-Dynamic Drag* (Hoerner, Midland Park NJ, 1965).
39. NOAA *U.S. Standard Atmosphere, 1976* (U.S. Govt Printing Office, Washington DC, 1976).
40. Chyba, C. F. *Icarus* **92**, 217–233 (1991).
41. Weissman, P. R. in *Global Catastrophes in Earth History* (eds Sharpton, V. L. & Ward, P. D.), 171–180 (Geol. Soc. Am. SP-247, Boulder CO, 1990).
42. Peale, S. J. *Icarus* **82**, 36–49 (1989).
43. Glasstone, S. & Dolan, P. J. *The Effects of Nuclear Weapons* (Dept of Defense, Washington DC 1977).
44. Jones, E. M. & Kodis, J. W. in *Geological Implications of Impacts of Large Asteroids and Comets on the Earth* (eds Silver, L. T. & Schultz, P. H.) 175–186 (Geol. Soc. Am. SP-190, Boulder CO, 1982).
45. ReVelle, D. O. *J. geophys. Res.* **81**, 1217–1230 (1976).